Vol 15 No 9, September 2006
1009-1963/2006/15(09)/2092-10

Chinese Physics

© 2006 Chin. Phys. Soc.
and IOP Publishing Ltd

Phonon spectrum and related thermodynamic properties of microcrack in bcc-Fe*

Cao Li-Xia(曹莉霞)[a)†] and Wang Chong-Yu(王崇愚)[a)b)c)]

[a)] *Central Iron and Steel Research Institute, Beijing* 100081, *China*
[b)] *International Centre for Materials Physics, Chinese Academy of Sciences, Shenyang* 110016, *China*
[c)] *Department of Physics, Tsinghua University, Beijing* 100084, *China*

(Received 22 March 2006; revised manuscript received 16 May 2006)

The phonon spectrum and the related thermodynamic properties of microcracks in bcc-Fe are studied with the recursion method by using the Finnis–Sinclair (F–S) N-body potential. The initial configuration of the microcracks is established from an anisotropic linear elastic solution and relaxed to an equilibrium by molecular dynamics method. It is shown that the local vibrational density of states of the atoms near a crack tip is considerably different from the bulk phonon spectrum, which is closely associated with the local stress field around the crack tip; meanwhile, the local vibrational energies of atoms near the crack tip are higher than those of atoms in a perfect crystal. These results imply that the crack tip zone is in a complex stress state and closely related to the structure evolution of cracks. It is also found that the phonon excitation is a kind of local effect induced by microcracks. In addition, the microcrack system has a higher vibrational entropy, which reflects the character of phonon spectrum related to the stress field induced by cracks.

Keywords: phonons, microcrack, metals
PACC: 6320

1. Introduction

Lattice vibrations have great influence on thermal, acoustic, electric, optical and mechanical properties of materials. The phonon spectrum, i.e. the frequency distribution of a vibrating system, is one of the important physical quantities which characterize the fundamental properties of a system.[1] In general, considering the periodicity of crystal, the phonon spectrum of a perfect crystal can be calculated by solving the secular equations.[2] This method is simple and straightforward for the study of perfect crystals, but it has disadvantages when solving for systems with defects or impurities. For a defect system, the recursion method[3] in real space becomes preferable, in which a group of new orthogonal base is introduced to make the general infinite eigenequations converted to tridiagonal infinite eigenequations in this new base representation. The local Green function can be expressed directly as the diagonal elements and nondiagonal elements, and used to calculate the local vibrational density of states (LDOS). Besides, the matrix elements after tridiagonalization have clear physical meanings.[4]

A great difference in vibrational property between perfect crystal and lattice defects, such as vacancy, impurity, dislocation, and grain boundary, etc, has been reported in many experimental measurements and theoretical calculations.[5−7] Defects existing in the real materials can bring on a significant change in thermodynamics property, for instance, free energy, vibrational entropy and heat capacity, which will affect the physical and mechanical properties of materials. Therefore, the lattice vibration and related thermodynamic properties of materials are of the most importance.[5−12]

In 1967 the lattice vibration frequency distribution of bcc-Fe was obtained by the neutron inelastic scattering experiments.[13−15] In addition, many relevant theoretical calculations have been also carried out. In the work of Masuda,[5] the LDOSs of atoms around the vacancies in bcc transition metals were calculated by using a tight-binding (TB) type electronic theory. Later, Wakayama *et al*[7] computed the LDOSs of segregated impurity and iron atoms at grain boundaries in bcc-Fe by the recursion method using an empirical atomic pair potential. These researches

*Project supported by the State Key Development Program for Basic Research of China (Grant No TG 2000067102) and the National Natural Science Foundation of China (Grant No 90306016).
†E-mail: cao_lx@sohu.com

show that material properties mainly depend on the local structure.

Irons and steel are important materials in industry. It has been observed that the actual fracture strength of iron is much lower than its theoretical value, which is attributed to the fact that the mechanical properties of metals are extremely sensitive to the microscopic structures of materials.[16] Hence the actual strength decrease of materials is closely related to the existence of defects. Microcracking in materials is one of the crucial factors which will lead to fracture. Considerable attention has been paid to the research of microcracks, which range from macroscopical scale to microscopical scale.[17−22]

In our work, by the use of the Finnis–Sinclair (F–S) N-body potential,[23,24] the dynamic matrix is constructed for the calculation of the phonon spectrum in a perfect crystal and defect system. The initial configuration of bcc-Fe (010) [101] microcrack is derived from the anisotropic linear elastic solution,[25] and the equilibrium structure is obtained by molecular dynamics (MD) method. The real space Green function method[26] is used to calculate the local properties of each atom in the crack tip zone, such as LDOS and local vibrational energy as well as other thermodynamic properties. By analysing these local properties, we have revealed that the existing microcracks may cause some atomic processes, such as atomic bond breaking, stacking faults and twins to occur in the crack tip.

2. Theoretical description and calculation model

2.1. The method of calculation

The F–S N-body potential is chosen in the MD because of its efficiency for the calculation of bcc metal, and the total energy of system can be determined by the potential as

$$U_{\rm tot} = U_{\rm N} + U_{\rm P}\,, \tag{1}$$

where $U_{\rm N}$ is the N-body term and $U_{\rm P}$ is the conventional central paired potential summation.

The interatomic force constants ϕ can be derived from the second derivation of the total energy

$$\phi_{ij\alpha\beta} = \frac{\partial^2 U}{\partial u_{i\alpha}\partial u_{j\beta}}\,, \tag{2}$$

where i and j are the number of atoms; α and β indicate the directions of atomic vibration.

In the harmonic approximation, we have the lattice vibration equation of the system as follows:

$$-m_i\ddot{u}_{i\alpha} = \sum_{j\beta}\phi_{ij\alpha\beta}u_{j\beta}\,. \tag{3}$$

Let

$$u_{i\alpha} = m_i^{-1/2}A_{i\alpha}{\rm e}^{-{\rm i}\omega t}\,, \tag{4}$$

then

$$\omega^2 A_{i\alpha} = \sum_{j\beta}(m_i m_j)^{-1/2}\phi_{ij\alpha\beta}A_{j\beta}\,. \tag{5}$$

Define the dynamical matrix

$$H_{ij\alpha\beta} = \frac{\phi_{ij\alpha\beta}}{\sqrt{m_i m_j}} \tag{6}$$

and use the matrix symbol, and Eq.(5) will become

$$\omega^2\cdot\boldsymbol{u} = H\cdot\boldsymbol{u}\,, \tag{7}$$

where ω^2 can be determined from the eigenequation

$$|H - I\omega^2| = 0\,. \tag{8}$$

The corresponding local Green function is

$$G_{l\,l}(\omega^2) = \langle l|\,(\omega^2 I - H)^{-1}|l\rangle\,, \tag{9}$$

where l is the location of atom, I is the unit matrix, ω is the frequency and H is the matrix composed of $H_{ij\alpha\beta}$.

The recursion method[27] is a real-space Green function approach, and it converts a complicated physical problem into a simple chain model. The chain model can be represented with a set of orthogonal basis functions $|u_i\rangle$ with two sets of parameters $\{a_n\}$, $\{b_n\}$. In the recursion method, we choose an appropriate base vector $|u_0\rangle$ to make the $G_{00}(\omega^2)$ represent a local Green function located at atom No.1 of the system. The recurrence relation describing the action of the Hamiltonian on the orbitals is

$$b_{n+1}|u_{n+1}\rangle = H|u_n\rangle - a_n|u_n\rangle - b_n|u_{n-1}\rangle\,. \tag{10}$$

With the relation (10) the dynamical matrix H can be tridiagonalized within the normal and orthogonal basis function $\{u_i\}$ as shown below:

$$H = \begin{bmatrix} a_0 & b_1 & & 0 \\ b_1 & a_1 & b_2 & \\ & b_2 & a_2 & \ddots \\ 0 & & \ddots & \ddots \end{bmatrix}. \tag{11}$$

The corresponding local Green function $G_{00}(\omega^2)$ is expanded in the continued fraction

$$G_{00}(\omega^2) = \cfrac{1}{\omega^2 - a_0 - \cfrac{b_1^2}{\omega^2 - a_1 - \cfrac{b_2^2}{\ddots}}} . \tag{12}$$

Based on the property of Green's function, the LDOS can be expressed as

$$\rho\,(\omega^2) = -\frac{1}{\pi} I_{\mathrm{m}} G_{00}(\omega^2)\,, \tag{13}$$

or

$$\rho(\omega) = 2\omega\rho(\omega^2)\,. \tag{14}$$

In order to calculate the infinite continued fraction, we truncate $G_{00}(\omega^2)$ at the l level. For the crystalline structure with a single kind of atom, a_l and b_l will rapidly converge to a_∞ and b_∞ respectively. In the self-consistent cutting off approximation,[4] one can have

$$a_\infty = H_{11} = a_0\,, \qquad b_\infty = \frac{1}{2} a_\infty\,. \tag{15}$$

Using the $\rho_i(\omega)$ function, we can also investigate the thermodynamic properties,[28]such as vibrational free energy F, specific heat C_v at constant volume and vibrational entropy S

$$F = 3rNkT \int_0^{\omega_L} \ln\Big\{2\sinh\Big(\frac{\hbar\omega}{2kT}\Big)\Big\}\rho(\omega)\mathrm{d}\omega, \tag{16}$$

$$C_v = 3rNk \int_0^{\omega_L} \Big(\frac{\hbar\omega}{2kT}\Big)^2 \mathrm{csch}^2\Big(\frac{\hbar\omega}{2kT}\Big)\rho(\omega)\,\mathrm{d}\omega, \tag{17}$$

$$S = 3rNk \int_0^{\omega_L} \Big[\frac{\hbar\omega}{2kT}\coth\Big(\frac{\hbar\omega}{2kT}\Big) - \ln\Big\{2\sinh\Big(\frac{\hbar\omega}{2kT}\Big)\Big\}\Big]\rho(\omega)\,\mathrm{d}\omega\,. \tag{18}$$

2.2. The models of calculation

For a perfect bcc-Fe crystal, the level l in recursion method is taken as a truncating length and its different values have been tested to calculate the vibrational spectrum $\rho_i(\omega)$. We find that the calculated $\rho_i(\omega)$ no longer changes significantly when l beyond 7, which means it is sufficient to obtain the accurate $\rho_i(\omega)$ if truncating is taken up to the seventh level.

Figure 1 describes the calculation models for the perfect crystal and the microcrack defect system, respectively. In the perfect crystal, for the specific atom i, there are 1695 atoms involved within the 7 levels, which are displayed in the region I in Fig.1(a). Since the F–S potential is cut off at the second neighbour and in order to eliminate the surface effect, the neighbouring atoms of the region I should be included in the calculation system. So, in total there are 20000 atoms in the system as shown in region II of Fig.1(a).

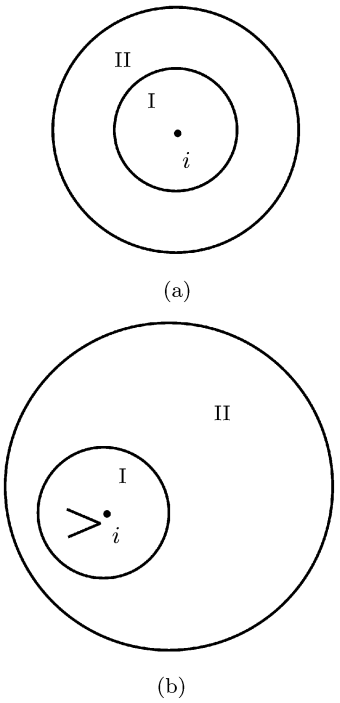


Fig.1. The calculation models: (a) perfect crystal for bcc-Fe; (b) defect system for bcc-Fe with microcracks.

For the microcrack system as shown in Fig.1(b), we mainly focus on the atoms in a crack tip zone. We know that in the recursion method, the specific atom i must be numbered as No.1 and then other atoms are numbered circling around it. It should be noted that in the defect system, the calculated atom i is near a defect but not in the centre of model. Comparing with the perfect system, the neighbouring atoms of the atom i have changed, consequentially affecting the atoms included in each level, which is shown in region I in Fig.1(b). Therefore, more atoms will be involved in the calculation system (region II in Fig.1(b)).

3. Results and discussion

3.1. Bulk phonon spectrum and related thermodynamic properties for bcc-Fe

Figure 2 shows the thermodynamic properties for the perfect bcc-Fe in the 0–800 K temperature range, obtained from the vibrational frequency distribution.

The calculated vibrational entropy S is presented in Fig.2(a). It is well known that the entropy includes the contributions from both electrons and phonons, and at high temperatures phonons play a main role for entropy. With temperature decreasing, the lattice vibration is gradually 'frozen', and the electrons contribution becomes dominant.

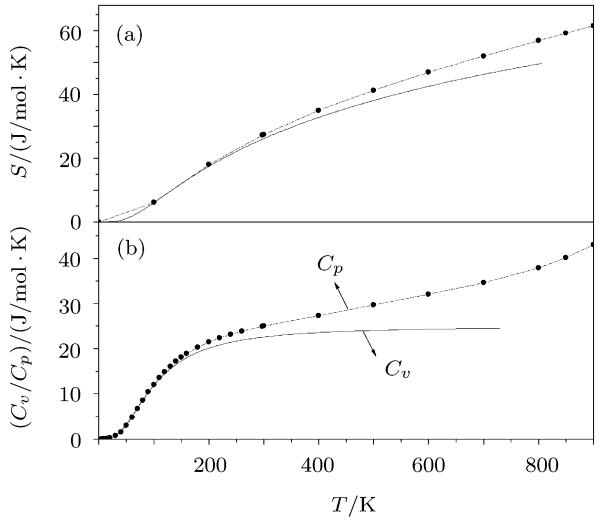


Fig.2. Thermodynamic properties of bcc-Fe within 0–800 K: (a) is for the vibrational entropy; (b) is for the specific heat. The solid lines represent the calculated values and the dash lines represent the experimental results.

As seen in Fig.2(a), within 100–650 K, the calculated entropy is in good agreement with the experimental value.[29] For the temperatures below 100 K, the calculated value decreases sharply down to zero, whereas the experimental value decreases smoothly. This discrepancy is attributed to the fact that in our calculation only the effect of phonons is considered while in experiments the electrons contribution is also included.

In Fig.2(b), for the temperatures above the room temperature, the calculated specific heat C_v at constant volume reaches a constant of 24 $J/(\text{mol}\cdot\text{K})$, which is exactly consistent with the value from Debye theory. For the temperatures below 100 K, the calculated C_v is close to the experimental value C_p.[29] This is because at low temperatures, the harmonic approximation can approximately describe the behaviour of real crystals.

Based on the above analyses we can conclude that the F–S potential is efficient for calculating the vibrational properties and the relevant thermodynamic properties for the bcc-Fe. Thus, we can use it further to obtain the vibrational properties of the defect system.

3.2. (010) [101] Fe microcrack

3.2.1. Configuration

The configuration of microcracks is initially constructed by the anisotropic linear elastic solution under opening mode loading.[25] It can be seen in experiment that the most prevalent cleavage planes are the {100} planes in α-Fe, and accordingly we choose the crystallographic orientation of cracks as the crack face on (010) plane and crack front along the [101] direction. This geometric model makes the $\langle 111\rangle$ {112} slip system available for activation.

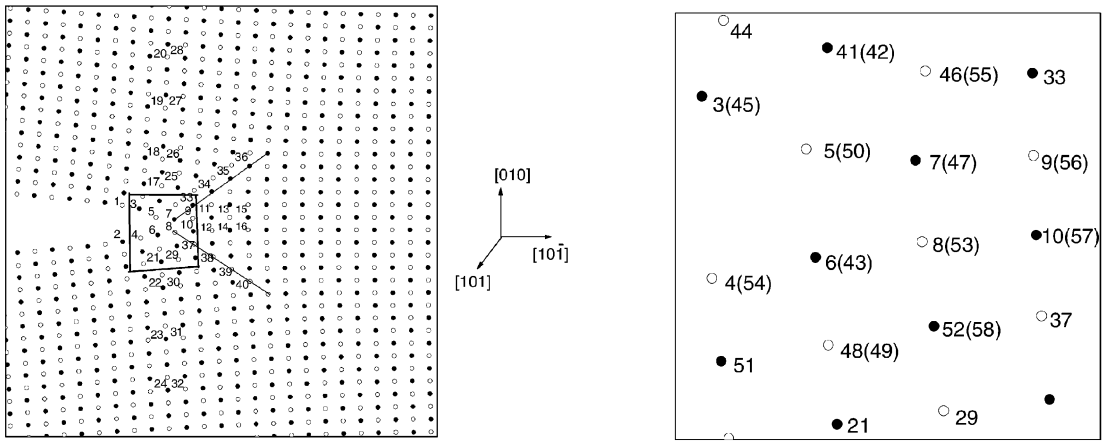


Fig.3. (a) Equilibrium atomic configuration of (010) [101] microcracks in bcc-Fe. The open circles represent atoms in layer A and the solid circles represent atoms in layer B; (b) The detailed atom numbers corresponding to the crack tip zone surrounded by the solid lines in Fig.3(a). The numbering in parenthesis represents the atom at the same position on the next layer.

The equilibrium atomic configuration of the (010) [101] microcracks is obtained by MD relaxation, with the boundary conditions fixed along [10$\bar{1}$] and [010] directions, and the periodic boundary conditions fixed along the crack front of [101] direction. Figure 3(a) shows the equilibrium atomic configuration in the crack tip region, in which the open circles and solid circles denote the different positions of the atoms projected onto a (101) plane, respectively. And Fig.3(b) gives the detailed atom numbers corresponding to the crack tip zone in the Fig.3(a).

3.2.2. Local vibrational density of state

The density of states is correlated with many physical quantities and reflects the intrinsic characteristics of phonon spectrum. Therefore, it is of great significance to learn the information of the density of states when one's attention is focused on the physical properties of systems. Figure 4 gives the LDOSs of the atoms near the crack tip region.

The calculated vibrational frequency distribution for a perfect bcc-Fe crystal is shown with solid lines in Fig.4. The shape of the curve and the magnitude of the frequency are almost the same as the results obtained from the neutron inelastic scattering experiments.[13−15]

Figure 4(a) is the LDOSs of the atoms on the crack surfaces. These LDOSs each have a high peak in a low frequency region, which is attributed to the atoms on the surfaces with less coordination numbers and then the feature of the atomic bonding is different from that of the atom in the bulk. Besides, these atoms possess the characters of oscillatory decay, which are related to the complex stress state on the crack surface.

The LDOSs of crack tip atoms are shown in Fig.4(b), from which we notice that the LDOS of atom No.5 has the highest peak in the low frequency region. It is known that the shape of LDOS is closely related to the stress fields around the defect.[7] By calculating the variation in spacing between neighbouring atoms (listed in Table 1), we can see that the variation in spacing between atom No.5 and its neighbouring atoms is larger than that between other atoms and their neighbouring atoms. Particularly, the spacing between atoms No.5 and No.4 can increase up to 0.5185 Å. The increased spacing, compared with the atom spacing in equilibrium (shown in Table 1), means that the stress state of atom corresponds to the tensile state and then can influence the vibrational state of phonon. With the spacing between the neighbouring atoms shortening and the coordination of atoms increasing, the peak of phonon spectrum shifts toward the higher frequencies. Therefore, the LDOSs of atoms No.7 and No.8 have different features of broad peak due to their atomic environments and the stress conditions (see Table 1 and Table 2). It should be noted that the difference in shape between the vibration spectra of the atoms is closely related to the local stress fields under which these atoms are in different vibration states.

In Fig.4(c) and Fig.4(d) we provide the LDOSs of the atoms along the crack extension direction of [10$\bar{1}$] in dislocation-free zone (DFZ). In the process of crack propagation, the interaction between the crack and the dislocation leads to the formation of an abnormal elastic area in front of the crack tip, which is generally called DFZ. Figures 4(e) and 4(f) are respectively for the LDOSs of atoms on ($\bar{1}$21) slip plane along the [11$\bar{1}$] slip direction and on (12$\bar{1}$) slip plane along the [1$\bar{1}\bar{1}$] slip direction. It is clearly seen that these LDOSs all have similar shapes and the sharp peaks appearing at $\nu = 4.8 \times 10^{13} - 5.5 \times 10^{13}$ Hz in the high frequency bands are about 25%–50% higher than those of the bulk phonon spectrum. Since the local density of states is correlated with the squared amplitude of the lattice wave, the higher peak means the larger squared amplitude of the lattice wave of the atoms, which reflects a strong interaction between these atoms on the slip planes and the crack defect. The further analysis also can be made from Table 2, in which the structural energies on sites and the component of stresses on the atoms near the crack tip zone are given. It presents that these atoms are in a higher stress field, which is closely related to the process of structure evolution in crack and might affect the mechanical properties of materials. When the crack system is under the applied load, the bonding between atoms with high vibrational amplitudes, located on the (010) crack plane, tends to break down and lead to brittle cleavage, and the atoms with high vibrational amplitudes on {112} slip plane can be related to the atomic slip behaviour and sequent generation of the stacking faults and twins. These predicted phenomena have been observed in experiments[30,31] and MD simulations[32] about dynamic cracks.

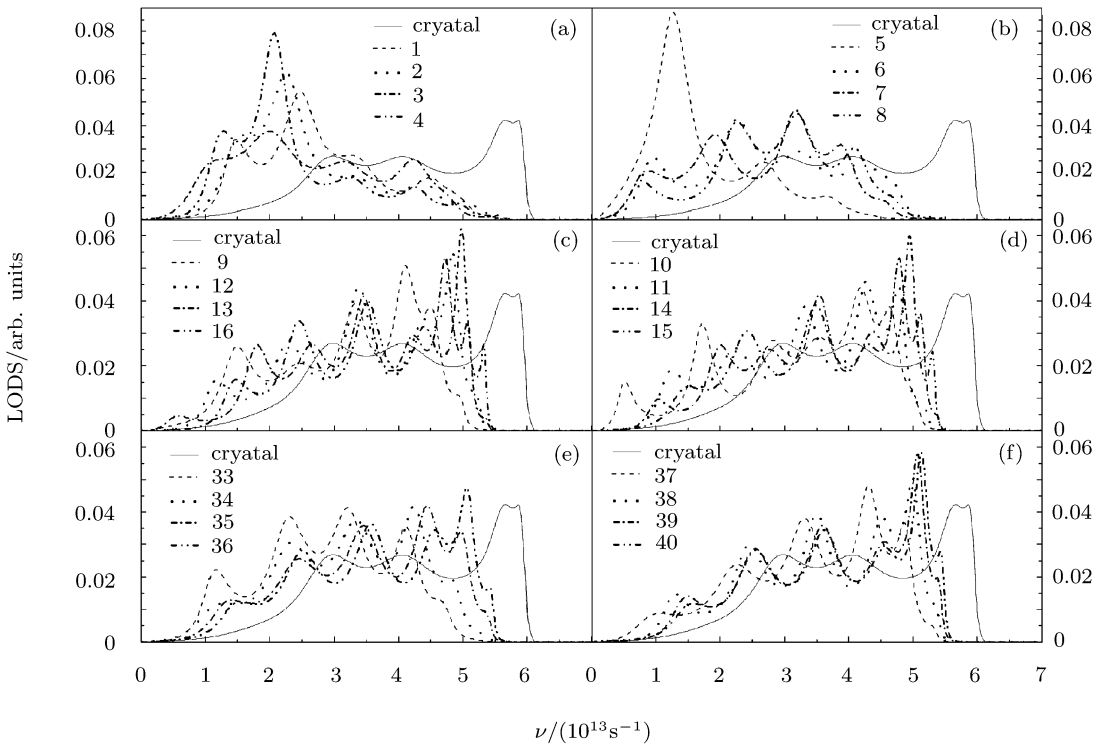


Fig.4. The LDOSs of atoms in crack tip zone: (a) on the crack surface; (b) the crack tip atoms; (c) and (d) along the propagation direction in the DFZ; (e) and (f) on the slip planes. The solid line shows the vibration frequency (ν) distribution for bcc-Fe perfect crystal.

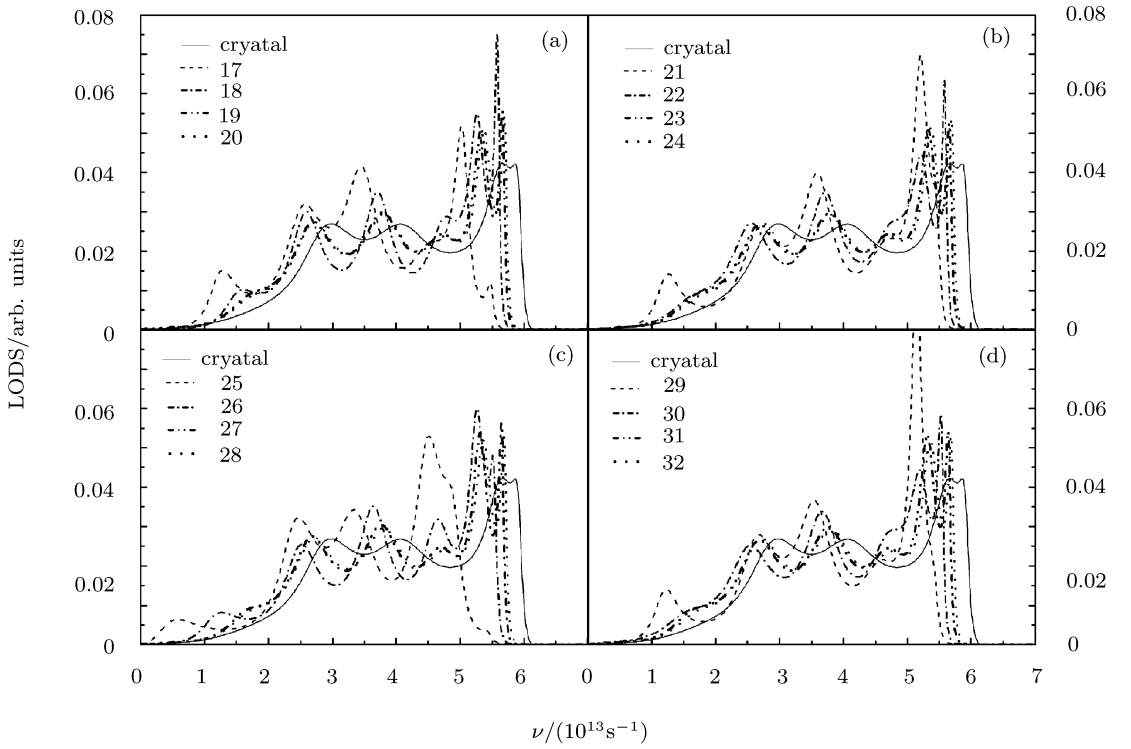


Fig.5. The LDOSs of atoms from No.17 to No.32 (shown in Fig.3(a)). The solid line shows the vibrational frequency (ν) distribution for bcc-Fe perfect crystal.

In addition, Fig.5 displays the LDOSs from atoms No.17 to No.32 (shown in Fig.3(a)). With the atoms being away from the crack tip, it is found that their LDOSs tend to the bulk spectrum. The local vibration of atoms becomes gradually weakened far from the crack tip, which reveals the local effect of phonon excitation induced by microcracks.

Table 1. The variation in spacing between crack tip atom and its neighbouring atoms (the atom number is shown in Fig.3(b)).

The numbering of atoms	The first neighbouring atoms (equilibrium spacing is $\sqrt{3}/2a$ and a is the lattice parameter of bcc Fe)		The second neighbouring atoms (equilibrium spacing is a)	
	the number of neighbouring atom	variation in spacing between atoms Δd/ Å	the number of neighbouring atom	variation in spacing between atoms Δd/Å
No.5	6	0.3897	3	0.1216
	4	0.5185	7	0.0645
	41	0.3269	45	0.1225
	44	0.3879	47	0.0648
	8	0.3032	0	
	43	0.3904	0	
	46	0.1977		
	42	0.3272		
No.6	5	0.3897	54	−0.0238
	49	0.1424	21	0.2938
	51	0.1598	53	−0.0041
	50	0.3899	4	−0.0238
	52	0.0889	8	−0.0038
	48	0.1425	0	
	7	0.1461		
	0			
No.7	53	0.0390	5	0.0645
	6	0.1461	50	0.0647
	55	0.1664	52	0.2337
	41	0.2509	56	0.1084
	10	0.1374	9	0.1082
	8	0.0392	0	
	33	0.2360		
	46	0.1669		
No.8	5	0.3032	6	−0.0038
	52	0.1018	29	0.3358
	48	0.1431	10	0.0932
	7	0.0392	43	−0.0045
	37	0.1637	46	0.3325
	58	0.1016	57	0.0930
	9	0.1641		
	47	0.0388		

Table 2. The components of stress of atoms and the structural energies on site E_l of atoms near crack tip zone.

the numbering of atoms	σ_{xx}/GPa	σ_{yy}/GPa	E_l/eV
No.5	7.884	8.407	−3.6960
No.6	3.937	5.031	−3.8992
No.7	6.14	3.451	−4.0498
No.8	5.747	4.767	−4.1163
No.9	4.873	3.611	−4.1248
No.10	4.430	3.553	−4.1681
No.33	5.360	3.883	−4.1397
No.37	3.673	3.583	−4.2238

3.2.3. Local vibrational energy

By using the LDOS of atoms, we calculate the local vibrational energy at the lattice of crystal. The local vibrational energy E_l is given by

$$E_l = \int_0^{\omega_L} \rho_l(\omega) \frac{\hbar\omega}{\exp(\hbar\omega/kT) - 1} \mathrm{d}\omega \,. \qquad (19)$$

The calculated local vibrational energies E_l of atoms near the crack tip zone at room temperature T = 296 K are shown in Fig.6. The energies of atoms No.5 and No.6 in crack tip are respectively 0.021 eV and 0.018 eV, which are much higher than those of atoms in a perfect crystal (0.014 eV). Figures 6(a) and 6(b) give the vibrational energies of atoms from No.17 to No.32 (shown in Fig.3(a)). It is found that with the atoms being away from the crack tip, their local vibrational energies gradually decrease and approach to those in the perfect crystal, which is reconciled with the LDOS result.

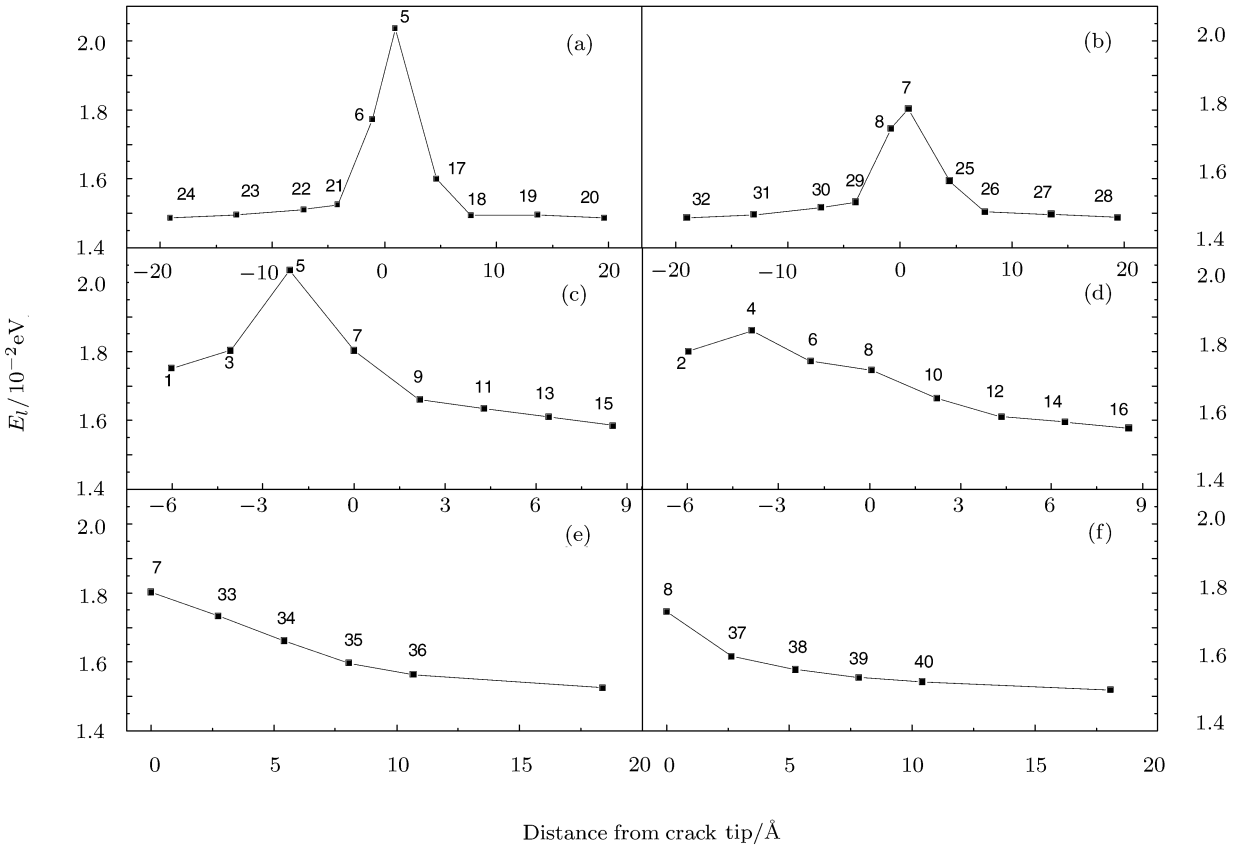


Fig.6. Local vibrational energy of atoms near crack tip zone.

Figures 6(c) and 6(d) present the local vibrational energies of atoms on the crack surface and atoms in the DFZ along the propagation direction. For the surface atoms (No.1–No.4), a reduction in coordination number makes the local vibrational energies of these atoms much higher than those in the perfect crystal.

For the atoms in the DFZ along the propagation direction, their local vibrational energies are also higher than those in the perfect crystal, which indicates that these atoms are unstable. It is possible for these atoms to break bonds under the applied stress field. Similarly, near the crack tip along the $\langle 111 \rangle$ slip direction on $\{112\}$ slip plane, the atoms have high local vibrational energies shown in Fig.6(e) and Fig.6(f), which implies that these atoms tend to slip and may induce the stacking faults and twins. All of these atomic behaviours constitute the general phenomena in the process of structure evolution in crack.

3.2.4. Vibrational entropy

From the LDOS of atoms, the local vibrational entropy can be calculated by Eq.(18). A local area around the crack tip is selected, including a total of 60 atoms in layer A and layer B. The calculated vibrational entropy in this area is 1838 J/(mol·K), which is 15 percent more than that in the perfect crystal including the same number of atoms. That is to say, the system with a microcrack has a high vibrational entropy compared with that in the perfect crystal. The state of high vibrational entropy shows the phonon effect to be related to the stress field induced by crack.

4. Summary

In this paper, the phonon spectrum and the related thermodynamic properties of microcracks in bcc-Fe have been studied with the recursion method, and the dynamic matrix is constructed based on the F–S N-body potential. Our calculation results have revealed that the LDOSs of the atoms near a crack tip zone are quite different from the bulk phonon spectrum. At the crack tip, the LDOSs of atoms each have a sharp peak in a low frequency region, which is closely related to the local stress field around the crack tip. On the other hand, the LDOSs of atoms along the propagation direction and slip direction in the DFZ have sharp peaks in a high frequency region, which indicates the strong interaction between these active atoms in the DFZ and the crack defect; meanwhile, the local vibrational energies of atoms in this region are much higher than those in a perfect crystal. The vibrational states of these atoms are closely related to the atomic behaviours in the crack system under an applied stress field, such as the bond breaking and structure evolution of the stacking faults and twinning.

It is observed that away from the crack tip, the LDOS and local vibrational energies of atoms tend to those of the perfect crystal, which reveals the local effect on phonon excitation created by microcracks.

Furthermore, the microcrack system has a higher vibrational entropy, which shows the phonon effect to be related to the stress field induced by cracks.

References

[1] Born M and Huang K 1954 *Dynamical Theory of Crystal Lattices* (Oxford: Clarendon)

[2] Callaway J 1974 *Quantum Theory of the Solid State* (New York: Academic) p1

[3] Haydock R 1980 *Solid State Physics* vol. 35, edited by Ehreinreich H, Seitz F and Turnbull D (New York: Academic) p215

[4] Wu S Y and Zheng Z B 1983 *Acta Phys. Sin.* **32** 46 (in Chinese)

[5] Masuda K 1982 *J. Physique* **43** 921

[6] Zheng Z B, Shao Z A and Wang C Y 1988 *J. Phys.* F:*Met. Phys.* **18** 1137

[7] Wakayama S, Hashinmoto M, Ishida Y, Yamamoto R and Doyama M 1984 *Acta Metall.* **32** 21

[8] Guo Y F, Zhang H F, Liu H B, Zhao D L and Wang C Y 2001 *Computat. Mater. Sci.* **20** 228

[9] An Z, Li Z J, Liu Y and Li Y C 2000 *Chin. Phys.* **9** 37

[10] Zhang H Q 2004 *Acta Phys. Sin.* **53** 1162 (in Chinese)

[11] Zhao F and Yuan L B 2005 *Acta Phys. Sin.* **54** 4511 (in Chinese)

[12] Liang X X and Ban S L 2004 *Chin. Phys.* **13** 71

[13] Brockhouse B N, Abou-Helal H E and Hallman E D 1967 *Solid State Commun.* **5** 211

[14] Bergsma J, Van Dijk C and Tocchetti D 1967 *Phys. Lett.* A **24** 270

[15] Minkiewicz V J, Shirane G and Nathans R 1967 *Phys. Rev.* **162** 528

[16] Feng D (Eds.) 1999 *Metal Physics* vol. **3** (Beijing: Science Press) p437 (in Chinese)

[17] Griffith A A 1920 *Philos. Trans. Roy. Soc.* A **221** 163

[18] Rice J R and Wang J S 1989 *Mater. Sci. Eng.* A **107** 23

[19] Gumbsch P, Riedle J, Hartmaier A and Fischmeister H F 1998 *Science* **282** 1293

[20] Buehler M J, Abraham F F and Gao H J 2003 *Nature* **426** 141

[21] Gross S P, Fineberg J, Maccormick W D and Swinney H L 1993 *Phys. Rev. Lett.* **71** 2417

[22] Sharon E, Gross S P and Fineberg J 1995 *Phys. Rev. Lett.* **74** 5096

[23] Finnis M W and Sinclair J E 1984 *Phil. Mag.* A **50** 45

[24] Finnis M W and Sinclair J E *Erratum* 1986 *Phil. Mag.* A **53** 161

[25] Sih G C and Liebowitz H (Eds.) 1968 *Fracture: An Advanced Treatise*, vol. **2** (New York: Academic Press) p67

[26] Economac E N 1979 *Green's Functions in Quantum Physics* (Berlin: Springer)

[27] Haydock R, Heine V and Kelly M J 1975 *J. Phys.* C **8** 2591

[28] Maradudin A A, Montroll E W and Weiss G H 1963 *Theory of Lattice Dynamics in the Harmonic Approximation* (NewYork: Academic) p46

[29] Baker H and Benjamin D (Eds.) 1979 *Metals Handbook* ninth ed., vol. 2 (Metals Park, OH: American Society for Metals) p750

[30] Hull D 1960 *Acta Metall.* **8** 11

[31] Bošanský J and Šmida T 2002 *Mater. Sci. Eng.* A **323** 198

[32] Machová A, Beltz G E and Chang M 1999 *Modelling Simul. Mater. Sci. Eng.* **7** 949